The 2016 World Congress on
Advances in Civil, Environmental, and Materials Research (ACEM16)
Jeju Island, Korea, August 28-September 1, 2016

Coupled thermoelectroelastic analysis of composite cylindrical shells with embedded piezoelectric sensors and actuators

*G. M. Kulikov[1], S. V. Plotnikova[2] and M. G. Kulikov[3]

[1), 2), 3)] *Laboratory of Intelligent Materials and Structures*
Tambov State Technical University, Sovetskaya, 106, 392000 Tambov, Russia
[1)] gmkulikov@mail.ru

ABSTRACT

This paper focuses on the implementation of the sampling surfaces (SaS) method for the three-dimensional coupled steady-state thermoelectroelastic analysis of layered composite shells with piezoelectric layers embedded into the shell. The SaS shell formulation is based on choosing inside the *n*th layer I_n SaS parallel to the middle surface in order to introduce the temperatures, electric potentials and displacements of these surfaces as basic shell variables. Such choice of unknowns with the consequent use of Lagrange polynomials of degree $I_n - 1$ in the assumed distributions of the temperature, electric potential, displacements and mechanical properties through the thickness of the layer leads to the robust thermopiezoelectric shell formulation. The inner SaS are located inside each layer at Chebyshev polynomial nodes that allows one to minimize uniformly the error due to Lagrange interpolation. As a result, the SaS formulation can be applied efficiently to analytical solutions for layered piezoelectric shells with embedded sensors and actuators, which asymptotically approach the three-dimensional exact solutions of thermopiezoelectricity as the number of SaS I_n tends to infinity.

1. INTRODUCTION

Three-dimensional (3D) analysis of layered piezoelectric plates and shells under thermal loading has received considerable attention during past twenty years (see, e.g. Wu 2008, 2016). There are at least five approaches to 3D exact solutions of thermoelectroelasticity for piezoelectric plates and shells, namely, the Pagano approach (Dube 1996, Shang 1997, Ootao 2000, Zhang 2002a, 2002b), the state space approach (Xu 1995, Tarn 2002, 2008, Vel 2003, Zhong 2005), the power series

---
[1)] Professor
[2)] Associate Professor
[3)] Research Scientist

expansion approach, i.e. the Frobenius method, (Xu 1995, Kapuria 1997a, 1997b, Ootao 2002a, 2002b), the asymptotic expansion approach (Cheng 2000), and the sampling surfaces (SaS) approach (Kulikov 2015a, 2015b, 2016).

In this paper, the SaS approach is utilized for the first time for the coupled thermoelectroelastic stress analysis of laminated composite shells with embedded piezoelectric sensors and actuators. According to the SaS approach (Kulikov 2012, 2013), we choose arbitrarily located surfaces inside the *n*th layer parallel to the middle surface of a shell $\Omega^{(n)1}, \Omega^{(n)2}, ..., \Omega^{(n)I_n}$ to introduce temperatures $T^{(n)1}, T^{(n)2}, ..., T^{(n)I_n}$, electric potentials $\varphi^{(n)1}, \varphi^{(n)2}, ..., \varphi^{(n)I_n}$ and displacement vectors $\mathbf{u}^{(n)1}, \mathbf{u}^{(n)2}, ..., \mathbf{u}^{(n)I_n}$ of these surfaces as basic shell variables, where I_n is the total number of SaS of the *n*th layer ($I_n \geq 3$). Such choice of temperatures, electric potentials and displacements with the consequent use of the Lagrange polynomials of degree $I_n - 1$ in the assumed distributions of the temperature, electric potential, displacements and mechanical properties through the thickness of the layer allows the presentation of governing equations of the SaS shell formulation in a very compact form.

It should be noticed that the SaS shell formulation with equally spaced SaS (Kulikov 2001, 2008, 2011) does not work properly with the Lagrange polynomials of high degree because of Runge's phenomenon (Burden 2010). This phenomenon yields the wild oscillation at the edges of the interval when the user deals with some specific functions similar to the shell metric functions. If the number of equispaced nodes is increased then the oscillations become even larger. However, the use of the Chebyshev polynomial nodes inside the shell body (Kulikov 2012, 2013) can help to improve significantly the behavior of the Lagrange polynomials of high degree because such a choice permits one to minimize uniformly the error due to the Lagrange interpolation. This fact gives an opportunity to obtain the stresses with a prescribed accuracy employing the sufficiently large number of SaS. It means in turn that the solutions based on the SaS concept *asymptotically* approach the 3D exact solutions of thermoelectroelasticity as $I_n \to \infty$.

2. DESCRIPTION OF DISPLACEMENT AND STRAIN FIELDS

Consider a layered shell of the thickness *h*. Let the middle surface Ω be described by orthogonal curvilinear coordinates θ_1 and θ_2, which are referred to the lines of principal curvatures of its surface. The thickness coordinate θ_3 is oriented in the normal direction. Introduce the following notations: $A_\alpha(\theta_1, \theta_2)$ are the coefficients of the first fundamental form; $\kappa_\alpha(\theta_1, \theta_2)$ are the principal curvatures of the middle surface; $c_\alpha = 1 + \kappa_\alpha \theta_3$ are the components of the shifter tensor; $c_\alpha^{(n)i_n}(\theta_1, \theta_2)$ are the components of the shifter tensor at SaS of the *n*th layer $\Omega^{(n)i_n}$ (Fig. 1) defined as

$$c_\alpha^{(n)i_n} = c_\alpha(\theta_3^{(n)i_n}) = 1 + \kappa_\alpha \theta_3^{(n)i_n}, \tag{1}$$

where $\theta_3^{(n)i_n}$ are the transverse coordinates of SaS given by

$$\theta_3^{(n)1} = \theta_3^{[n-1]}, \qquad \theta_3^{(n)I_n} = \theta_3^{[n]},$$

$$\theta_3^{(n)m_n} = \frac{1}{2}(\theta_3^{[n-1]} + \theta_3^{[n]}) - \frac{1}{2}h^{(n)} \cos\left(\pi \frac{2m_n - 3}{2(I_n - 2)}\right), \tag{2}$$

where $\theta_3^{[n-1]}$ and $\theta_3^{[n]}$ are the transverse coordinates of layer interfaces $\Omega^{[n-1]}$ and $\Omega^{[n]}$; $h^{(n)} = \theta_3^{[n]} - \theta_3^{[n-1]}$ is the thickness of the *n*th layer. It is worth noting that the transverse coordinates of inner SaS $\theta_3^{(n)m_n}$ coincide with coordinates of the Chebyshev polynomial nodes. This fact has a great meaning for a convergence of the SaS method (Kulikov 2012, 2013).

Here, the index *n* identifies the belonging of any quantity to the *n*th layer and runs from 1 to *N*, where *N* is the number of layers; the index m_n identifies the belonging of any quantity to the inner SaS of the *n*th layer and runs from 2 to $I_n - 1$; the indices i_n, j_n, k_n describe all SaS of the *n*th layer and run from 1 to I_n; Latin tensorial indices i, j, k, l range from 1 to 3; Greek indices α, β range from 1 to 2.

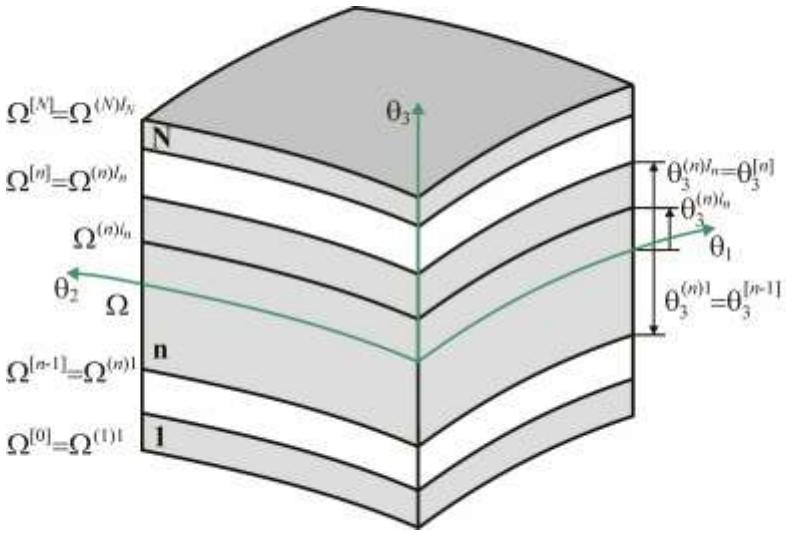

Fig. 1 Geometry of the laminated shell

We start now with the first two assumptions of the proposed layered piezoelectric shell formulation. Let us assume that the displacement and strain fields are distributed through the thickness of the *n*th layer as

$$u_i^{(n)} = \sum_{i_n} L^{(n)i_n} u_i^{(n)i_n}, \qquad \theta_3^{[n-1]} \le \theta_3 \le \theta_3^{[n]}, \tag{3}$$

$$\varepsilon_{ij}^{(n)} = \sum_{i_n} L^{(n)i_n} \varepsilon_{ij}^{(n)i_n}, \qquad \theta_3^{[n-1]} \le \theta_3 \le \theta_3^{[n]}, \tag{4}$$

where $u_i^{(n)i_n}(\theta_1,\theta_2)$ and $\varepsilon_{ij}^{(n)i_n}(\theta_1,\theta_2)$ are the displacements and strains of SaS of the *n*th layer $\Omega^{(n)i_n}$; $L^{(n)i_n}(\theta_3)$ are the Lagrange polynomials of degree $I_n - 1$ given by

$$u_i^{(n)i_n} = u_i(\theta_3^{(n)i_n}), \tag{5}$$

$$\varepsilon_{ij}^{(n)i_n} = \varepsilon_{ij}(\theta_3^{(n)i_n}), \tag{6}$$

$$L^{(n)i_n} = \prod_{j_n \ne i_n} \frac{\theta_3 - \theta_3^{(n)j_n}}{\theta_3^{(n)i_n} - \theta_3^{(n)j_n}}. \tag{7}$$

The strains of SaS of the *n*th layer in terms of displacements of SaS are expressed as

$$2\varepsilon_{\alpha\beta}^{(n)i_n} = \frac{1}{c_\beta^{(n)i_n}} \lambda_{\alpha\beta}^{(n)i_n} + \frac{1}{c_\alpha^{(n)i_n}} \lambda_{\beta\alpha}^{(n)i_n},$$

$$2\varepsilon_{\alpha 3}^{(n)i_n} = \frac{1}{c_\alpha^{(n)i_n}} \lambda_{3\alpha}^{(n)i_n} + \beta_\alpha^{(n)i_n}, \quad \varepsilon_{33}^{(n)i_n} = \beta_3^{(n)i_n}, \tag{8}$$

where $\lambda_{i\alpha}^{(n)i_n}$ are the strain parameters of SaS of the *n*th layer (Kulikov 2013); $\beta_i^{(n)i_n} = u_{i,3}(\theta_3^{(n)i_n})$ are the values of the derivative of displacements with respect to thickness coordinate on SaS defined as

$$\lambda_{\alpha\alpha}^{(n)i_n} = \frac{1}{A_\alpha} u_{\alpha,\alpha}^{(n)i_n} + B_\alpha u_\beta^{(n)i_n} + k_\alpha u_3^{(n)i_n},$$

$$\lambda_{\beta\alpha}^{(n)i_n} = \frac{1}{A_\alpha} u_{\beta,\alpha}^{(n)i_n} - B_\alpha u_\alpha^{(n)i_n},$$

$$\lambda_{3\alpha}^{(n)i_n} = \frac{1}{A_\alpha} u_{3,\alpha}^{(n)i_n} - k_\alpha u_\alpha^{(n)i_n} \quad \text{for} \quad \beta \ne \alpha, \tag{9}$$

$$\beta_i^{(n)i_n} = \sum_{j_n} M^{(n)j_n}(\theta_3^{(n)i_n}) u_i^{(n)j_n}, \tag{10}$$

where $M^{(n)j_n} = L^{(n)j_n}_{,3}$ are the derivatives of Lagrange polynomials, which are calculated at SaS as follows:

$$M^{(n)j_n}(\theta_3^{(n)i_n}) = \frac{1}{\theta_3^{(n)j_n} - \theta_3^{(n)i_n}} \prod_{k_n \neq i_n, j_n} \frac{\theta_3^{(n)i_n} - \theta_3^{(n)k_n}}{\theta_3^{(n)j_n} - \theta_3^{(n)k_n}} \quad \text{for} \quad j_n \neq i_n,$$

$$M^{(n)i_n}(\theta_3^{(n)i_n}) = -\sum_{j_n \neq i_n} M^{(n)j_n}(\theta_3^{(n)i_n}). \tag{11}$$

It is seen from Eq. (10) that the key functions $\beta_i^{(n)i_n}$ of the layered shell formulation are represented as a linear combination of displacements of SaS of the *n*th layer $u_i^{(n)j_n}$.

3. DESCRIPTION OF ELECTRIC FIELD

Next, we introduce the third and fourth assumptions of the proposed layered thermopiezoelectric shell formulation. Let the electric potential and the electric field be distributed through the thickness of the *n*th layer similar to Eqs. (3,4):

$$\varphi^{(n)} = \sum_{i_n} L^{(n)i_n} \varphi^{(n)i_n}, \quad \theta_3^{[n-1]} \leq \theta_3 \leq \theta_3^{[n]}, \tag{12}$$

$$E_i^{(n)} = \sum_{i_n} L^{(n)i_n} E_i^{(n)i_n}, \quad \theta_3^{[n-1]} \leq \theta_3 \leq \theta_3^{[n]}, \tag{13}$$

where $\varphi^{(n)i_n}(\theta_1, \theta_2)$ are the electric potentials of SaS of the *n*th layer; $E_i^{(n)i_n}(\theta_1, \theta_2)$ are the components of the electric field at SaS of the *n*th layer defined as

$$\varphi^{(n)i_n} = \varphi(\theta_3^{(n)i_n}), \tag{14}$$

$$E_i^{(n)i_n} = E_i(\theta_3^{(n)i_n}). \tag{15}$$

The electric field on SaS of the *n*th layer in terms of electric potentials of SaS is given by

$$E_\alpha^{(n)i_n} = -\frac{1}{A_\alpha c_\alpha^{(n)i_n}} \varphi_{,\alpha}^{(n)i_n}, \tag{16}$$

$$E_3^{(n)i_n} = -\sum_{j_n} M^{(n)j_n}(\theta_3^{(n)i_n}) \varphi^{(n)j_n}. \tag{17}$$

As can be seen from Eq. (17), the normal components of the electric field on SaS of the *n*th layer $E_3^{(n)i_n}$ are represented as a linear combination of electric potentials of SaS of the same layer $\varphi^{(n)j_n}$.

4. DESCRIPTION OF TEMPERATURE FIELD

The following step consists in a choice of the suitable approximation of the temperature and temperature gradient through the thickness of the layer. It is apparent that the temperature and temperature gradient distributions should be chosen similar to Eqs. (3,4) and Eqs. (12,13). Therefore, the next two assumptions of the proposed layered thermopiezoelectric shell formulation are

$$T^{(n)} = \sum_{i_n} L^{(n)i_n} T^{(n)i_n}, \quad \theta_3^{[n-1]} \le \theta_3 \le \theta_3^{[n]}, \tag{18}$$

$$\Gamma_i^{(n)} = \sum_{i_n} L^{(n)i_n} \Gamma_i^{(n)i_n}, \quad \theta_3^{[n-1]} \le \theta_3 \le \theta_3^{[n]}, \tag{19}$$

where $T^{(n)i_n}(\theta_1,\theta_2)$ are the temperatures of SaS of the *n*th layer; $\Gamma_i^{(n)i_n}(\theta_1,\theta_2)$ are the components of the temperature gradient on SaS of the *n*th layer defined as

$$T^{(n)i_n} = T(\theta_3^{(n)i_n}), \tag{20}$$

$$\Gamma_i^{(n)i_n} = \Gamma_i(\theta_3^{(n)i_n}). \tag{21}$$

The components of the temperature gradient on SaS of the *n*th layer in terms of temperatures of SaS are expressed as

$$\Gamma_\alpha^{(n)i_n} = \frac{1}{A_\alpha c_\alpha^{(n)i_n}} T_{,\alpha}^{(n)i_n}, \tag{22}$$

$$\Gamma_3^{(n)i_n} = \sum_{j_n} M^{(n)j_n}(\theta_3^{(n)i_n}) T^{(n)j_n}. \tag{23}$$

It is seen from Eq. (23) that the normal components of the temperature gradient at SaS of the *n*th layer $\Gamma_3^{(n)i_n}$ are represented again as a linear combination of temperatures of SaS of same layer $T^{(n)j_n}$.

5. CONSTITUTIVE EQUATIONS

As constitutive equations, we accept the Fourier heat conduction equations

$$q_i^{(n)} = -k_{ij}^{(n)} \Gamma_j^{(n)}, \quad \theta_3^{[n-1]} \le \theta_3 \le \theta_3^{[n]}, \tag{24}$$

where $k_{ij}^{(n)}$ are the thermal conductivities of the nth layer. Here and in the following developments, the summation on repeated Latin indices is implied.

Introduce the seventh assumption of the thermal layered shell formulation. Assume that the thermal conductivity coefficients are distributed through the thickness of the nth layer as follows:

$$k_{ij}^{(n)} = \sum_{i_n} L^{(n)i_n} k_{ij}^{(n)i_n}, \quad \theta_3^{[n-1]} \le \theta_3 \le \theta_3^{[n]} \tag{25}$$

that is extensively utilized in this paper, where $k_{ij}^{(n)i_n} = k_{ij}^{(n)}\left(\theta_3^{(n)i_n}\right)$ are the values of the thermal conductivity tensor on SaS of the nth layer.

For simplicity, we consider the case of linear piezoelectric materials. Therefore, the constitutive equations are expressed as

$$\sigma_{ij}^{(n)} = C_{ijkl}^{(n)} \varepsilon_{kl}^{(n)} - e_{kij}^{(n)} E_k^{(n)} - \gamma_{ij}^{(n)} \Theta^{(n)},$$

$$D_i^{(n)} = e_{ikl}^{(n)} \varepsilon_{kl}^{(n)} + \in_{ik}^{(n)} E_k^{(n)} + r_i^{(n)} \Theta^{(n)},$$

$$\eta^{(n)} = \gamma_{kl}^{(n)} \varepsilon_{kl}^{(n)} + r_k^{(n)} E_k^{(n)} + \chi^{(n)} \Theta^{(n)}, \tag{26}$$

where $\Theta^{(n)} = T^{(n)} - T_0$ is the temperature rise of the nth layer; T_0 is the reference temperature; $C_{ijkl}^{(n)}$ are the elastic constants; $e_{kij}^{(n)}$ are the piezoelectric constants; $\gamma_{ij}^{(n)}$ are the thermal stress coefficients; $\in_{ik}^{(n)}$ are the dielectric constants; $r_i^{(n)}$ are the pyroelectric constants; $\chi^{(n)}$ is the entropy-temperature coefficient given by

$$\chi^{(n)} = \rho^{(n)} c_{\mathrm{v}}^{(n)} / T_0, \tag{27}$$

where $\rho^{(n)}$ and $c_{\mathrm{v}}^{(n)}$ are the mass density and the specific heat per unit mass.

Finally, we introduce the last assumption of the SaS thermopiezoelectric shell formulation. Let the material constants be distributed through the thickness of the nth layer as accepted throughout this paper

$$\Xi^{(n)} = \sum_{i_n} L^{(n)i_n} \Xi^{(n)i_n}, \quad \theta_3^{[n-1]} \le \theta_3 \le \theta_3^{[n]}, \tag{28}$$

$$\Xi^{(n)} = [C_{ijkl}^{(n)},\, e_{ijk}^{(n)},\, \gamma_{ij}^{(n)},\, \in_{ij}^{(n)},\, r_i^{(n)},\, \rho^{(n)},\, c_{\mathrm{v}}^{(n)}],$$

where $\Xi^{(n)i_n} = \Xi^{(n)}(\theta_3^{(n)i_n})$ are the values of material constants on SaS of the *n*th layer.

6. ANALYTICAL SOLUTION FOR LAYERED COMPOSITE CYLINDRICAL SHELL

In this section, we study a layered composite cylindrical shell with embedded piezoelectric layers subjected to thermal and electro-mechanical loads. The boundary conditions for the simply supported shell with electrically grounded edges maintained at the reference temperature are written as

$$\Theta^{(n)} = \varphi^{(n)} = \sigma_{11}^{(n)} = u_2^{(n)} = u_3^{(n)} = 0 \text{ at } \theta_1 = 0 \text{ and } \theta_1 = L, \tag{29}$$

where θ_1 is the longitudinal coordinate; L is the length of the shell. To satisfy the boundary conditions, Eq. (29), we search the analytical solution by a method of the double Fourier series expansion

$$\Theta^{(n)i_n} = \sum_{r=1}^{\infty}\sum_{s=0}^{\infty} \Theta_{rs}^{(n)i_n} \sin\frac{r\pi\theta_1}{L}\cos s\theta_2, \tag{30}$$

$$\varphi^{(n)i_n} = \sum_{r=1}^{\infty}\sum_{s=0}^{\infty} \varphi_{rs}^{(n)i_n} \sin\frac{r\pi\theta_1}{L}\cos s\theta_2, \tag{31}$$

$$u_1^{(n)i_n} = \sum_{r=1}^{\infty}\sum_{s=0}^{\infty} u_{1rs}^{(n)i_n} \cos\frac{r\pi\theta_1}{L}\cos s\theta_2, \tag{32}$$

$$u_2^{(n)i_n} = \sum_{r=1}^{\infty}\sum_{s=0}^{\infty} u_{2rs}^{(n)i_n} \sin\frac{r\pi\theta_1}{L}\sin s\theta_2, \tag{33}$$

$$u_3^{(n)i_n} = \sum_{r=1}^{\infty}\sum_{s=0}^{\infty} u_{3rs}^{(n)i_n} \sin\frac{r\pi\theta_1}{L}\cos s\theta_2, \tag{34}$$

where θ_2 is the circumferential coordinate; *r, s* are the wave numbers. The external electromechanical loads are also expanded in double Fourier series.

Substituting Eq. (30) in a variational equation of the heat conduction theory, we obtain the systems of linear algebraic equations in terms of temperature rises $\Theta_{rs}^{(n)i_n}$ of order K, where $K = \sum_n I_n - N + 1$. Therefore, the temperature rises of SaS can be found using a method of Gaussian elimination.

Substituting next Eqs. (31-34) in a variational equation of the thermopiezoelectric shell theory, one obtains the systems of linear algebraic equations in terms of $\Theta_{rs}^{(n)i_n}$, $\varphi_{rs}^{(n)i_n}$, $u_{1rs}^{(n)i_n}$, $u_{2rs}^{(n)i_n}$ and $u_{3rs}^{(n)i_n}$ of order 4*K* because the temperature rises of SaS are already known. These linear systems are solved again through the method of Gaussian elimination.

The described algorithm was performed with the Symbolic Math Toolbox, which incorporates symbolic computations into the numeric environment of MATLAB. This permits the obtaining of analytical solutions for layered composite cylindrical shells with embedded piezoelectric layers in the framework of the SaS thermoelectroelastic shell formulation, which asymptotically approach the 3D exact solutions of thermopiezoelectricity as the number of SAS of the *n*th layer I_n tends to infinity.

7. NUMERICAL EXAMPLES

Consider first a three-layer symmetric cross-ply cylindrical shell with the stacking sequence [90/0/90] composed of the graphite-epoxy composite and covered with two piezoelectric PVDF layers on its bottom and top surfaces. Thus, the hybrid five-layer cylindrical shell [PVDF/90/0/90/PVDF] with ply thicknesses $[3h_0/8h_0/8h_0/8h_0/3h_0]$ is studied, where $h_0 = h/30$. The material properties of the PVDF polarized in the thickness direction are taken to be (Kapuria 1997a):

$$E_1 = E_2 = E_3 = 2\,\text{GPa}, \quad \nu_{12} = \nu_{23} = \nu_{31} = 1/3,$$

$$\alpha_{11} = \alpha_{22} = \alpha_{33} = 120 \times 10^{-6}\,1/\text{K}, \quad k_{11} = k_{22} = k_{33} = 0.24\ \text{W/mK},$$

$$d_{311} = 3 \times 10^{-12}\,\text{m/V}, \quad d_{322} = 23 \times 10^{-12}\,\text{m/V}, \quad d_{333} = -30 \times 10^{-12}\,\text{m/V},$$

$$\in_{11} = \in_{22} = 3.078 \times 10^{-11}\,\text{F/m}, \quad \in_{33} = 3.141 \times 10^{-11}\,\text{F/m}, \quad r_3 = -27 \times 10^{-6}\,\text{C/m}^2\text{K},$$

where E_i are the elastic moduli; ν_{ij} are the Poisson's ratios; α_{ij} are the thermal coefficients of expansion; d_{ijk} are the piezoelectric moduli. The material properties of the graphite-epoxy composite are chosen as follows (Kapuria 1997b):

$$E_\text{L} = 172.5\,\text{GPa}, \quad E_\text{T} = 6.9\,\text{GPa}, \quad G_\text{LT} = 3.45\,\text{GPa}, \quad G_\text{TT} = 1.38\,\text{GPa}, \quad \nu_\text{LT} = \nu_\text{TT} = 0.25,$$

$$\alpha_\text{L} = 0.57 \times 10^{-6}\,1/\text{K}, \quad \alpha_\text{T} = 35.6 \times 10^{-6}\,1/\text{K}, \quad k_\text{L} = 36.42\ \text{W/mK}, \quad k_\text{T} = 0.96\ \text{W/mK},$$

$$\in_\text{L} = 3.095 \times 10^{-11}\,\text{F/m}, \quad \in_\text{T} = 2.653 \times 10^{-11}\,\text{F/m},$$

where L and T denote the fiber and transverse directions. To evaluate the entropy, we accept $\rho = 1780\,\text{kg/m}^3$, $c_\text{v} = 1400\,\text{J/kgK}$ and $\rho = 1800\,\text{kg/m}^3$, $c_\text{v} = 900\,\text{J/kgK}$ for the PVDF and graphite-epoxy, respectively.

The shell is subjected to sinusoidally distributed temperature loading on the top surface, whereas the bottom surface is maintained at the reference temperature. The bottom and top surfaces are electroded and grounded. Therefore, the boundary conditions can be written as

$$\Theta^+ = \Theta_0 \sin\frac{\pi\theta_1}{L}, \quad \varphi^+ = \sigma_{13}^+ = \sigma_{23}^+ = \sigma_{33}^+ = 0,$$
$$\Theta^- = \varphi^- = \sigma_{13}^- = \sigma_{23}^- = \sigma_{33}^- = 0, \tag{35}$$

where $\Theta_0 = 1\text{K}$ and $T_0 = 293\,\text{K}$. The geometric parameters of the shell are chosen to be $R = 1\text{m}$ and $L = 4\,\text{m}$, where R is the radius of the middle surface. It is supposed that the interfaces between the piezoelectric layers and the substrate are electroded and grounded.

To compare the results derived with the 3D exact solution of thermoelectroelasticity (Kapuria 1997b), we introduce dimensionless variables at crucial points as follows:

$$\overline{\Theta} = \Theta(L/2, z)/\Theta_0, \quad \overline{\varphi} = 10^3 d_\text{r}\varphi(L/2, z)/h\alpha_\text{r}\Theta_0,$$

$$\overline{u}_1 = 100u_1(0, z)/R\alpha_\text{r}\Theta_0, \quad \overline{u}_3 = 10u_3(L/2, z)/R\alpha_\text{r}\Theta_0,$$

$$\overline{q}_3 = 100hq_3(L/2, z)/k_\text{r}\Theta_0, \quad \overline{\eta} = 10^{-3}\eta(L/2, z)/E_\text{r}\alpha_\text{r}^2\Theta_0,$$

$$\overline{\sigma}_{13} = 10S\sigma_{13}(0, z)/E_\text{r}\alpha_\text{r}\Theta_0, \quad \overline{\sigma}_{33} = 10S\sigma_{33}(L/2, z)/E_\text{r}\alpha_\text{r}\Theta_0,$$

where $z = \theta_3/h$ is the dimensionless thickness coordinate; $S = R/h$ is the slenderness ratio; $E_\text{r} = 6.9\,\text{GPa}$, $\alpha_\text{r} = 35.6\times10^{-6}\,1/\text{K}$, $k_\text{r} = 36.42$ W/mK and $d_r = 30\times10^{-12}$ m/V are the representative moduli of the shell.

Figs. 2,3 display the distributions of the temperature, electric potential, displacements, heat flux, entropy and stresses through the thickness of the hybrid layered cylindrical shell for different values of the slenderness ratio employing seven SaS for each layer. A comparison with the 3D exact solution (Kapuria 1997b) is also presented. These results demonstrate convincingly the high potential of the developed SaS formulation because the boundary conditions on bottom and top surfaces of the shell for transverse stresses and the continuity conditions for a heat flux and transverse stresses at interfaces are satisfied exactly.

Next, we study a simply supported metal-ceramic cylindrical shell covered with the graphite-epoxy layer and PVDF at the bottom. Therefore, we deal here with a hybrid three-layer shell [PVDF/Graphite-Epoxy/Metal-Ceramic] with ply thicknesses [0.1*h*/0.1*h*/0.8*h*]. The metal-ceramic shell is made of the two-phase composite. The metal phase is aluminum with $E_{\mathrm{m}} = 7\times10^{10}\,\mathrm{Pa}$, $v_{\mathrm{m}} = 0.3$, $\alpha_{\mathrm{m}} = 23.4\times10^{-6}\,1/\mathrm{K}$, $k_{\mathrm{m}} = 233\,\mathrm{W/mK}$, $\in_{\mathrm{m}}=1.594\times10^{-11}\,\mathrm{F/m}$, $\rho_{\mathrm{m}} = 2707\,\mathrm{kg/m^3}$ and $c_{\mathrm{m}} = 896\,\mathrm{J/kgK}$; the thermal barrier is a SiC ceramic with $E_{\mathrm{c}} = 38\times10^{10}\,\mathrm{Pa}$, $v_{\mathrm{c}} = 0.17$, $\alpha_{\mathrm{c}} = 4.3\times10^{-6}\,1/\mathrm{K}$, $k_{\mathrm{c}} = 65\,\mathrm{W/mK}$, $\in_{\mathrm{c}}= 8.606\times10^{-11}\,\mathrm{F/m}$, $\rho_{\mathrm{c}} = 3100\,\mathrm{kg/m^3}$ and $c_{\mathrm{c}} = 670\,\mathrm{J/kgK}$. It is assumed that the material properties are varied through the thickness according to the rule of mixtures:

$$E = E_{\mathrm{m}}V_{\mathrm{m}} + E_{\mathrm{c}}V_{\mathrm{c}}, \quad v = v_{\mathrm{m}}V_{\mathrm{m}} + v_{\mathrm{c}}V_{\mathrm{c}}, \quad \alpha = \alpha_{\mathrm{m}}V_{\mathrm{m}} + \alpha_{\mathrm{c}}V_{\mathrm{c}},$$

$$k = k_{\mathrm{m}}V_{\mathrm{m}} + k_{\mathrm{c}}V_{\mathrm{c}}, \quad \in=\in_{\mathrm{m}} V_{\mathrm{m}}+ \in_{\mathrm{c}} V_{\mathrm{c}}, \quad \rho c = \rho_{\mathrm{m}}c_{\mathrm{m}}V_{\mathrm{m}} + \rho_{\mathrm{c}}c_{\mathrm{c}}V_{\mathrm{c}}, \tag{36}$$

where V_{m} and V_{c} are the volume fractions of metal and ceramic phases defined as

$$V_{\mathrm{m}} = 1 - V_{\mathrm{c}}, \quad V_{\mathrm{c}} = \left[(z+0.3)/0.8\right]^{\gamma}, \quad z \in [-0.3,\ 0.5], \tag{37}$$

where γ is the material gradient index; $z = \theta_3 / h$ is the dimensionless thickness coordinate.

Let us investigate a cylindrical shell subjected to sinusoidally distributed temperature loading on the top surface and consider the following boundary conditions:

$$\Theta^{+} = \Theta_0 \sin\frac{\pi\theta_1}{L}\cos 2\theta_2, \quad D_3^{+} = \sigma_{11}^{+} = u_2^{+} = u_3^{+} = 0,$$

$$\Theta^{-} = 0, \quad D_3^{-} = \sigma_{11}^{-} = u_2^{-} = u_3^{-} = 0, \tag{38}$$

where $\Theta_0 = 1\mathrm{K}$ and $T_0 = 293\,\mathrm{K}$. The interface between PVDF and graphite-epoxy is electroded and grounded.

To analyze the obtained results efficiently, we introduce dimensionless variables at crucial points as functions of the thickness coordinate as

$$\overline{\Theta} = \Theta(L/2,0,z)/\Theta_0, \quad \overline{q}_3 = 100hq_3(L/2,0,z)/k_{\mathrm{r}}\Theta_0,$$

$$\overline{\varphi} = d_{\mathrm{r}}\varphi(L/2,0,z)/h\alpha_{\mathrm{r}}\Theta_0, \quad \overline{D}_3 = S^2 D_3(L/2,0,z)/d_r E_{\mathrm{r}}\alpha_r\Theta_0,$$

$$\overline{u}_1 = 10^{-4}u_1(0,0,z)/R\alpha_{\mathrm{r}}\Theta_0, \quad \overline{u}_3 = 10^{-5}u_3(L/2,0,z)/R\alpha_{\mathrm{r}}\Theta_0,$$

$$\overline{\sigma}_{11} = 10^{-5}\sigma_{11}(L/2,0,\ z)/E_{\mathrm{r}}\alpha_{\mathrm{r}}\Theta_r, \quad \overline{\sigma}_{22} = 10^{-5}\sigma_{22}(L/2,0,z)/E_{\mathrm{r}}\alpha_{\mathrm{r}}\Theta_0,$$

$$\overline{\sigma}_{12} = 10^{-4}S\sigma_{12}(0,\pi/4,z)/E_{\mathrm{r}}\alpha_{\mathrm{r}}\Theta_0, \quad \overline{\sigma}_{13} = 10^{-3}S\sigma_{13}(0,0,z)/E_{\mathrm{r}}\alpha_{\mathrm{r}}\Theta_0,$$

$$\bar{\sigma}_{23} = 10^{-3} S\sigma_{23}(L/2, \pi/4, z)/E_{\mathrm{r}}\alpha_{\mathrm{r}}\Theta_0, \quad \bar{\sigma}_{33} = 10^{-3} S\sigma_{33}(L/2, 0, z)/E_{\mathrm{r}}\alpha_{\mathrm{r}}\Theta_0, \quad S = R/h,$$

where $E_{\mathrm{r}}, \alpha_{\mathrm{r}}, k_{\mathrm{r}}$ and d_r are the representative moduli taken from a previous example. The geometric parameters of a shell are chosen as $R = 1\mathrm{m}$ and $L = 4\mathrm{m}$.

Figs. 4,5 show the through-thickness distributions of the temperature, heat flux, electric potential, electric displacement, displacements and stresses for different values of the slenderness ratio S and material gradient index $\gamma = 2$ using 13 SaS for each layer. These results demonstrate again the high potential of the developed SaS shell formulation because the boundary conditions on bottom and top surfaces for transverse components of the electric displacement and stresses and the continuity conditions for transverse components of the heat flux and stresses at interfaces are satisfied properly.

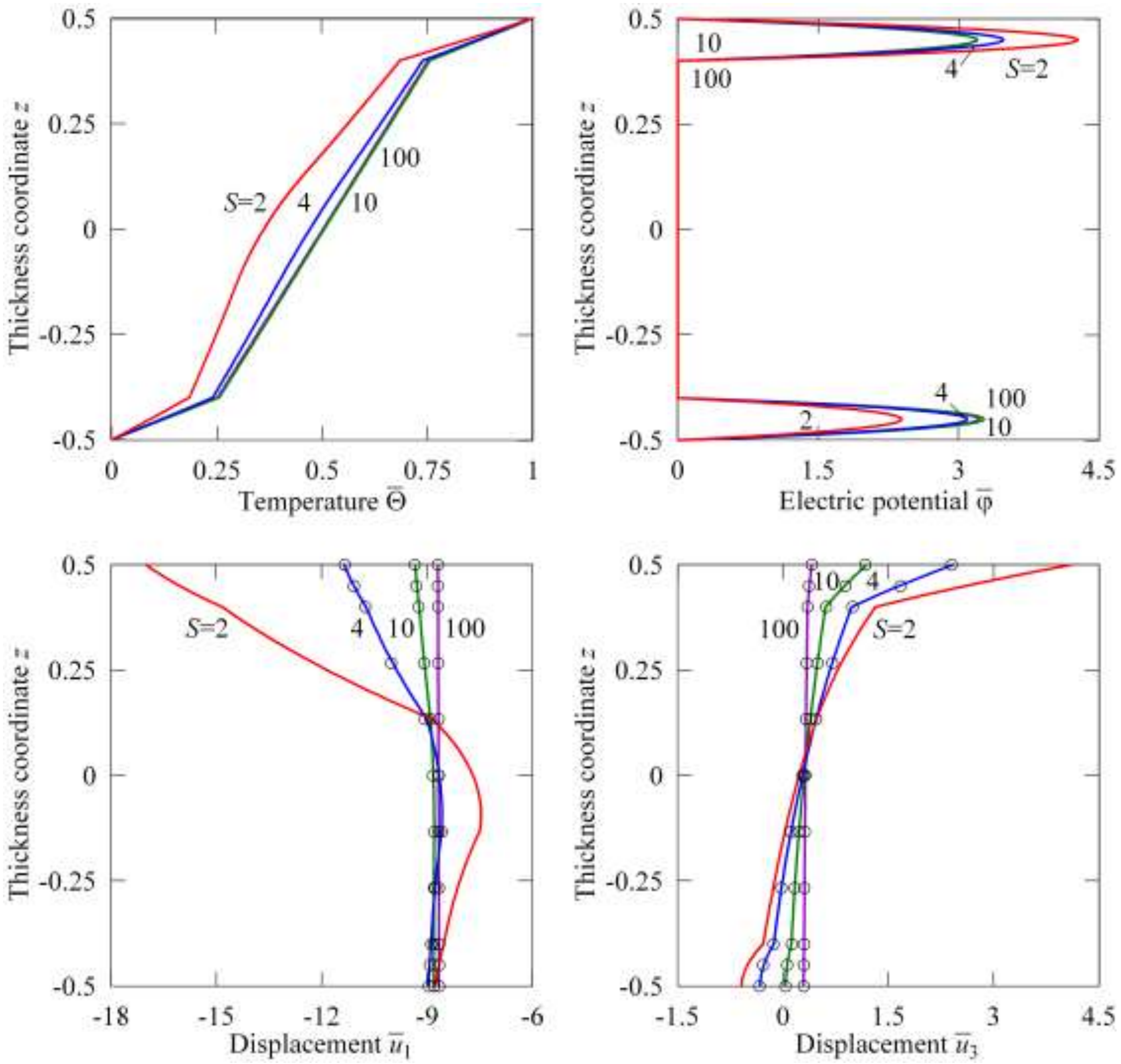

Fig. 2 Through-thickness distributions of the temperature, electric potential and displacements for a hybrid five-layer cylindrical shell: SaS formulation for $I_1 = I_2 = I_3 = I_4 = I_5 = 7$ and 3D exact solution (○) (Kapuria 1997b)

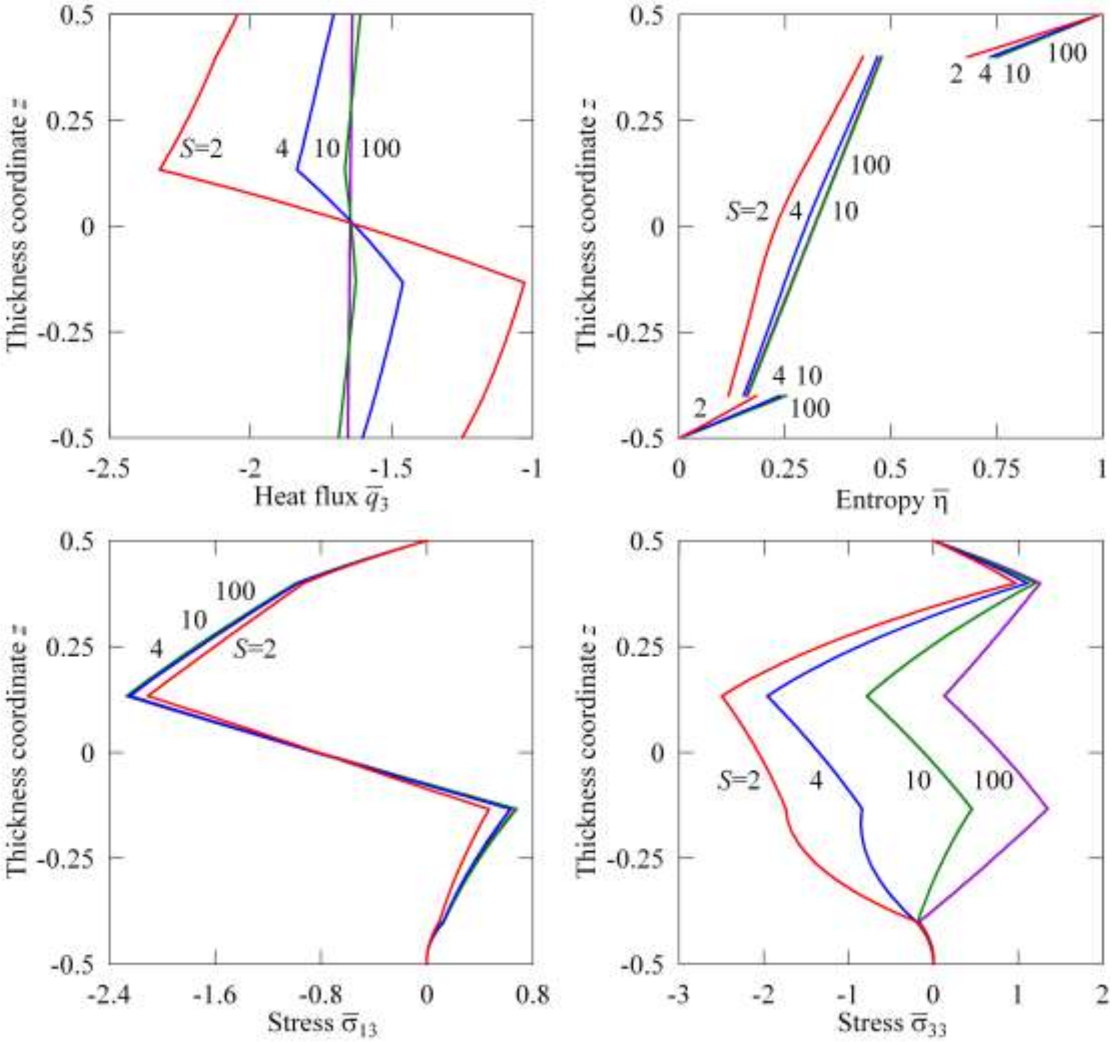

Fig. 3 Through-thickness distributions of the heat flux, entropy and stresses for a hybrid five-layer cylindrical shell: SaS formulation for $I_1 = I_2 = I_3 = I_4 = I_5 = 7$

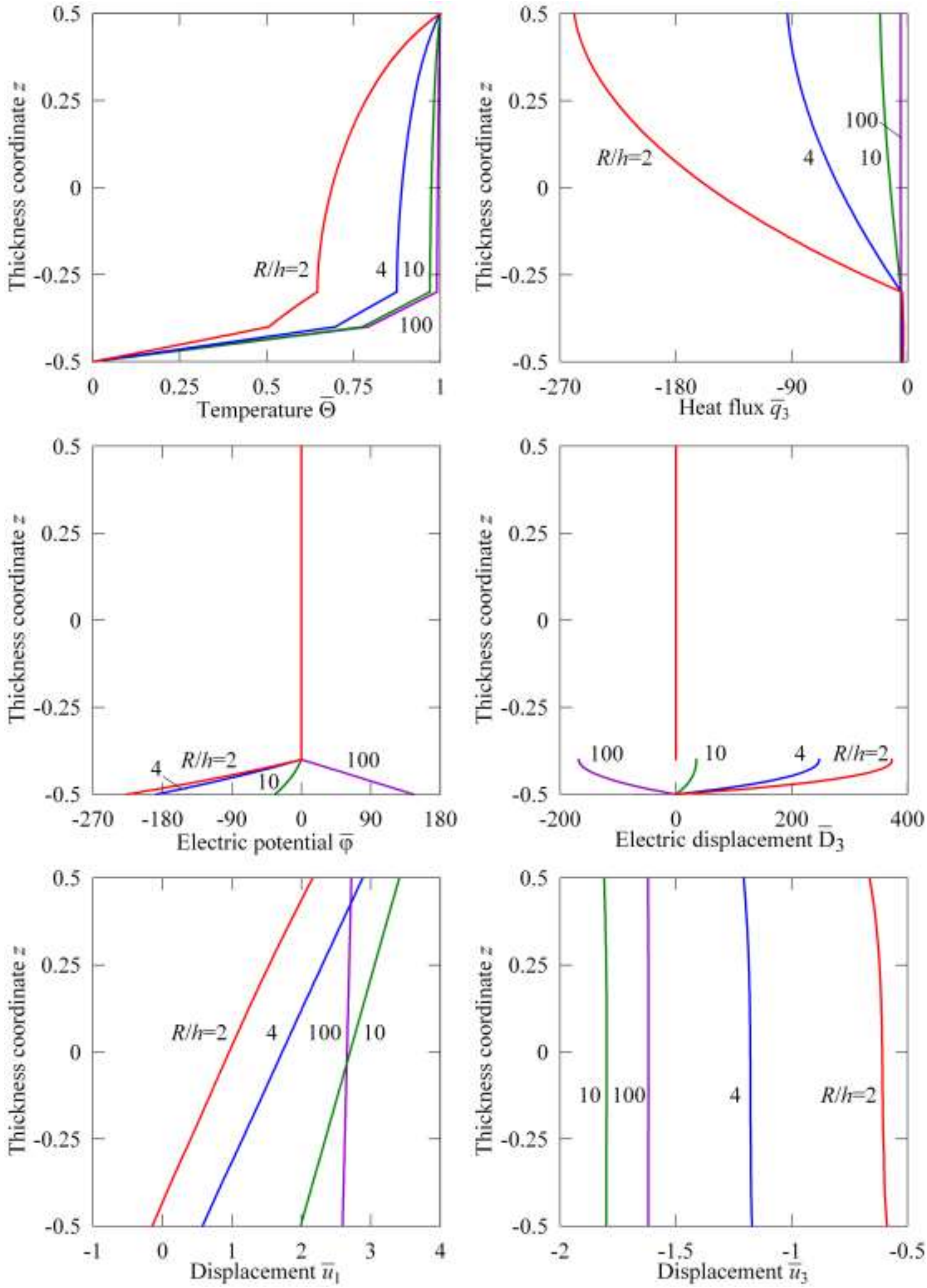

Fig. 4 Through-thickness distributions of the temperature, heat flux, electric potential, electric displacement and displacements for a hybrid three-layer cylindrical shell: SaS formulation for $\gamma = 2$ and $I_1 = I_2 = I_3 = 13$

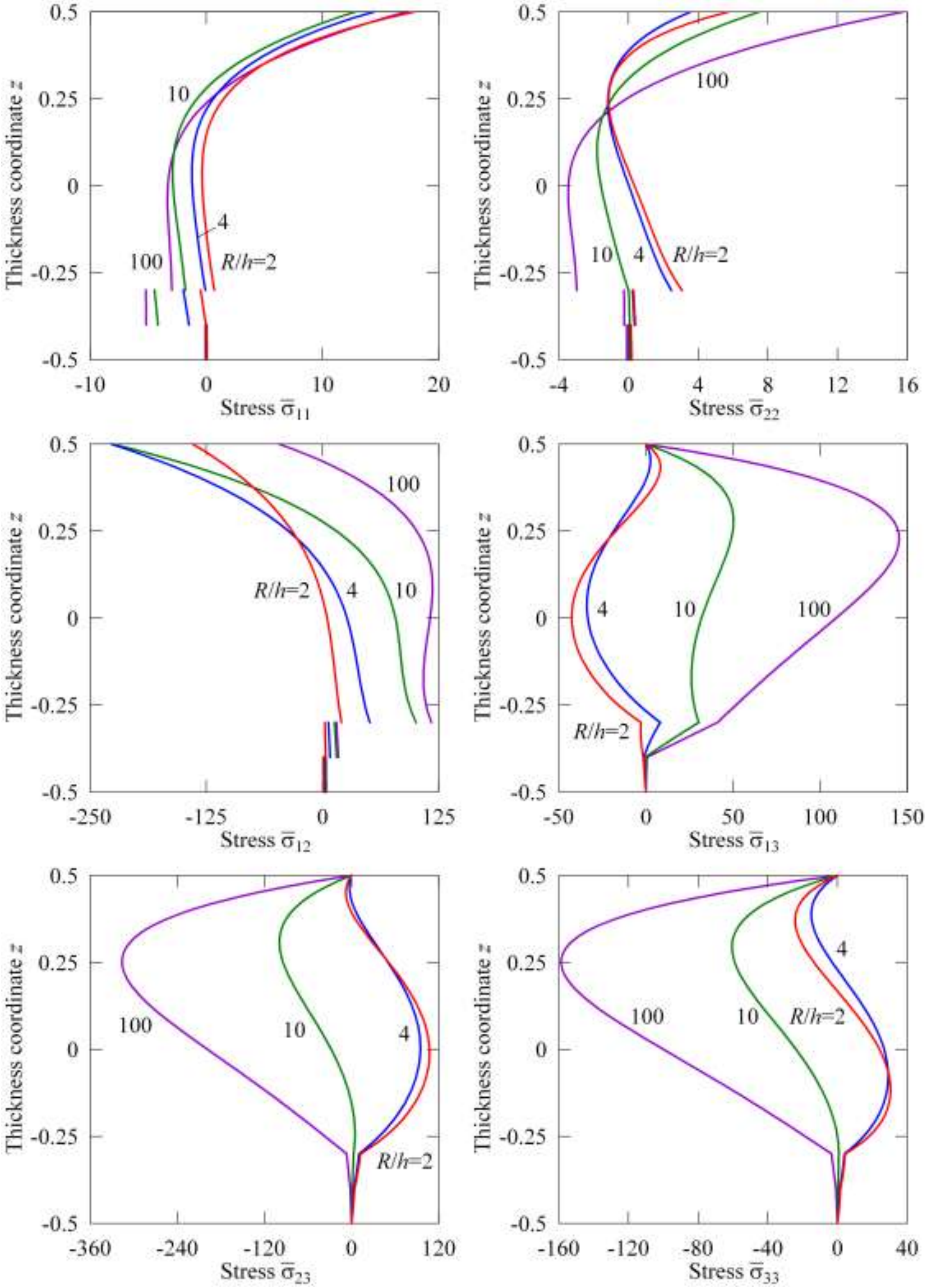

Fig. 5 Through-thickness distributions of stresses for a hybrid three-layer cylindrical shell: SaS formulation for $\gamma = 2$ and $I_1 = I_2 = I_3 = 13$

7. CONCLUSIONS

A robust SaS formulation for the coupled steady-state thermal stress analysis of layered piezoelectric shells has been proposed. It is based on a new concept of SaS located at Chebyshev polynomial nodes throughout the layers and interfaces as well. As a result, the developed SaS formulation gives an opportunity to obtain the Ritz solutions for layered cylindrical shells with embedded piezoelectric sensors and actuators with a prescribed accuracy, which can asymptotically approach the 3D exact solutions of thermopiezoelectricity as the number of SaS goes to infinity.

REFERENCES

Burden, R.L. and Faires, J.D. (2010), *Numerical Analysis*, (9th Edition), Brooks/Cole, Cengage Learning, Boston, USA.

Cheng, Z.Q. and Batra, R.C. (2000), “Three-dimensional asymptotic scheme for piezothermoelastic laminates”, *J. Therm. Stress*, **23**, 95–110.

Dube, G.P., Kapuria, S. and Dumir, P.C. (1996), “Exact piezothermoelastic solution of simply-supported orthotropic flat panel in cylindrical bending”, *Int. J. Mech. Sci.*, **38**, 1161–1177.

Kapuria, S., Dumir, P.C. and Sengupta, S. (1997a), “An exact axisymmetric solution for a simply supported piezoelectric cylindrical shell”, *Arch. Appl. Mech.*, **67,** 260–273.

Kapuria, S., Sengupta, S. and Dumir, P.C. (1997b), “Three-dimensional solution for a hybrid cylindrical shell under axisymmetric thermoelectric load”, *Arch. Appl. Mech.*, **67**, 320–330.

Kulikov, G.M. (2001), “Refined global approximation theory of multilayered plates and shells”, *J. Eng. Mech.*, **127**, 119–125.

Kulikov, G.M. and Carrera, E. (2008), “Finite deformation higher-order shell models and rigid-body motions”, *Int. J. Solids Struct.*, **45**, 3153–3172.

Kulikov, G.M. and Plotnikova, S.V. (2011), “On the use of a new concept of sampling surfaces in a shell theory”, *Adv. Structured Mater.*, **15**, 715–726.

Kulikov, G.M. and Plotnikova, S.V. (2012), “On the use of sampling surfaces method for solution of 3D elasticity problems for thick shells”, *ZAMM – J. Appl. Math. Mech.*, **92**, 910–920.

Kulikov, G.M. and Plotnikova, S.V. (2013), “Advanced formulation for laminated composite shells: 3D stress analysis and rigid-body motions”, *Compos. Struct.*, **95**, 236–246.

Kulikov, G.M. and Plotnikova, S.V. (2015a), “Exact 3D thermoelectroelastic analysis of piezoelectric plates through a sampling surfaces method”, *Mech. Adv. Mater. Struct*., **22,** 33–43.

Kulikov, G.M., Mamontov, A.A. and Plotnikova, S.V. (2015b), “Coupled thermoelectroelastic stress analysis of piezoelectric shells”, *Compos. Struct.*, **124**, 65–76.

Kulikov, G.M. and Plotnikova, S.V. (2016), “An analytical approach to three-dimensional coupled thermoelectroelastic analysis of functionally graded piezoelectric plates”, *J. Intel. Mater. Systems Struct.*, **17**, http://dx.doi.org/10.1177/1045389X15588627.

Ootao, Y. and Tanigawa, Y. (2000), "Three-dimensional transient piezothermoelasticity for a rectangular composite plate composed of cross-ply and piezoelectric laminae", *Int. J. Eng. Sci.*, **38**, 47–71.

Ootao, Y. and Tanigawa, Y. (2002a), "Transient piezothermoelasticity for a cylindrical composite panel composed of cross-ply and piezoelectric laminae", *Int. J. Mech. Sci.*, **44**, 1861–1877.

Ootao, Y. and Tanigawa, Y. (2002b), "Transient piezothermoelasticity for a cylindrical composite panel composed of angle-ply and piezoelectric laminae", *Int. J. Solids Struct.*, **39**, 5737–5752.

Shang, F., Wang, Z. and Li, Z. (1997), "Analysis of thermally induced cylindrical flexure of laminated plates with piezoelectric layers", *Compos. Part B*, **28**, 185–193.

Tarn, J.Q. (2002), "A state space formalism for piezothermoelasticity", *Int. J. Solids Struct.*, **39**, 5173–5184.

Tarn, J.Q. and Chang, H.H. (2008), "A refined state space formalism for piezothermoelasticity", *Int. J. Solids Struct.*, **45**, 3021–3032.

Vel, S.S. and Batra, R.C. (2003), "Generalized plane strain thermopiezoelectric analysis of multilayered plates", *J. Therm. Stress*, **26**, 353–377.

Wu, C.P., Chiu, K.H. and Wang, Y.M. (2008), "A review on the three-dimensional analytical approaches of multilayered and functionally graded piezoelectric plates and shells", Comput. Mater. Continua, **8**, 93–132.

Wu, C.P. and Liu, Y.C. (2016), "A review of semi-analytical numerical methods for laminated composite and multilayered functionally graded elastic/piezoelectric plates and shells", Compos. Struct., **147**, 1–15.

Xu, K, Noor, A.K. and Tang, Y.Y. (1995), "Three-dimensional solutions for coupled thermoelectroelastic response of multilayered plates", *Comput. Meth. Appl. Mech. Eng.*, **126**, 355–371.

Xu, K. and Noor, A.K. (1996), "Three-dimensional analytical solutions for coupled thermo-electroelastic response of multilayered cylindrical shells", *AIAA J.*, **34**, 802–810.

Zhang, C., Di, S. and Zhang, N. (2002a), "A new procedure for static analysis of thermo-electric laminated composite plates under cylindrical bending", *Compos. Struct.*, **56**, 131–140.

Zhang, C., Cheung, Y.K., Di, S. and Zhang, N. (2002b), "The exact solution of coupled thermoelectroelastic behavior of piezoelectric laminates". *Comput. Struct.*, **80**, 1201–1212.

Zhong, Z. and Shang, E.T. (2005), "Exact analysis of simply supported functionally graded piezothermoelectric plates", *J. Intel. Mater. Systems Struct.*, **16**, 643–651.